# Suppressed Dissociation of $H_2^+$ Vibrational States by Reduced Dipole Coupling

J. McKenna, F. Anis, B. Gaire, Nora G. Johnson, M. Zohrabi, K. D. Carnes, B. D. Esry, and I. Ben-Itzhak

*J. R. Macdonald Laboratory, Department of Physics, Kansas State University, Manhattan, Kansas 66506, USA*

(Received 24 June 2009; published 3 September 2009)

The suppression of $H_2^+$ strong-field dissociation has intrigued experimentalists and theorists since the early days of laser-molecular science. We unravel a vibrational suppression effect due to weak dipole-matrix element coupling strengths of certain vibrational states, dependent on the laser frequency—a form of Cooper minima. This effect is demonstrated by our full-dimensional calculations on $H_2^+$ dissociation and persists for a broad range of laser conditions including both weak and strong-field dissociation. Using a crossed-beams coincidence, three-dimensional momentum-imaging technique, the vibrational suppression effect is clearly observed for $H_2^+$ and $HD^+$ at 790 and 395 nm, in good agreement with our theory.

DOI: 10.1103/PhysRevLett.103.103006 PACS numbers: 33.80.Wz, 42.50.Hz

Intense ultrashort laser pulses are used to initiate, image, and control molecular dynamics and have many applications in molecular science [1]. Our understanding of strong-field molecular behavior has been built upon years of studying laser-driven processes in simple molecules like $H_2^+$ and $H_2$ [2]. We report here a seemingly forgotten molecular phenomenon that is exemplified for $H_2^+$—the suppression of dissociation of certain vibrational states caused by weak dipole-matrix element coupling. The concept of dipole-matrix elements is common to physics textbooks [3]. Yet, surprisingly, it has been overlooked in the strong-field laser community in favor of more exotic explanations of suppressed dissociation of $H_2^+$. Perhaps the most remarkable result we find is that much of the dynamics of $H_2^+$ can be qualitatively understood rather well using first-order perturbation theory without the need to invoke more complex intense-field dynamics.

One notable example can be found in the prolonged discussion on suppressed dissociation of $H_2^+$ [4–12]. Much of the excitement stems from the prediction of vibrational stabilization, which relates to the surprising theoretical result that some vibrational states have higher survival probabilities with increasing laser intensity [5,6]—in analogy to stabilization in atoms [13]. Although first suggested several decades ago [4], to our knowledge, vibrational stabilization has never been experimentally observed for $H_2^+$, and, in fact, calculations show that nuclear rotation strongly inhibits the stabilization process [6,7]. A mechanism that was first summoned to explain stabilization is vibrational trapping [8]. In trapping, population in high vibrational states is shelved in a laser-induced potential well, typically above the one-photon crossing in the adiabatic Floquet picture (light-dressed states, e.g., [14]). The trapping shelters the population from one-photon bond-softening [15–17] until after the pulse, when it may be released back into the bound $H_2^+$ $1s\sigma_g$ electronic state—thereby suppressing dissociation of those states. Trapping has also been used to interpret the observation of other phenomena such as below-threshold dissociation [9,10]. A second stabilization phenomenon, referring to stabilization as a function of wavelength and for a coherent initial vibrational wave packet, is dynamical dissociation quenching [11]. However, it too has never been observed experimentally and, as with intensity-dependent stabilization, is generally destroyed by nuclear rotation [12].

The fact that neither of these stabilization phenomena appears in calculations that include nuclear rotation is a strong indication that both phenomena are artifacts of one-dimensional theoretical models. Furthermore, many of the symptoms typically associated with the related mechanism of vibrational trapping, such as the reduced dissociation probability of certain vibrational states, can alternatively be explained by the suppression effect presented in this Letter. The suppression demonstrated here for $H_2^+$ using theory and experiment is a manifestation of the well-known Cooper minima effect [18] ubiquitous to photoabsorption studies. Essentially, the dipole-matrix elements of the $H_2^+$ vibrational states for a one-photon electronic transition oscillate in strength as a function of laser frequency $\omega$.

To understand how the dipole-matrix elements cause a suppression in $H_2^+$, as we briefly remarked on in Ref. [7], we plot the square of their amplitude, $|D_v(E)|^2$, for each vibrational state $v$ as a function of the dissociation kinetic energy release (KER) in Fig. 1(b). The dipole-matrix elements can be written as $D_v(E) = \langle F_E^{\alpha'}(R)|D_{\alpha\alpha'}(R)|F_v^{\alpha}(R)\rangle$, where $F(R)$ are the nuclear wave functions as a function of internuclear distance, $E$ is the energy of the final continuum state (KER $= E + 13.6$ eV), $v$ the initial vibrational state, $\alpha$ and $\alpha'$ the initial ($1s\sigma_g$) and final ($2p\sigma_u$) electronic states, and $D_{\alpha\alpha'}(R) = \langle \Phi_{\alpha'}(\mathbf{R};\mathbf{r})|z|\Phi_{\alpha}(\mathbf{R};\mathbf{r})\rangle \sim R/2$, where $\Phi$ is the Born-Oppenheimer electronic basis (see Ref. [7]). The structured dips in $|D_v(E)|^2$ in Fig. 1(b) result from poor overlap of the continuum wave function with the bound wave function as a function of $\omega$, as pictorially shown for $v = 9$ in Fig. 1(a)—the overlap is better for 790 and 450 nm than for 570 nm. Comparison

 

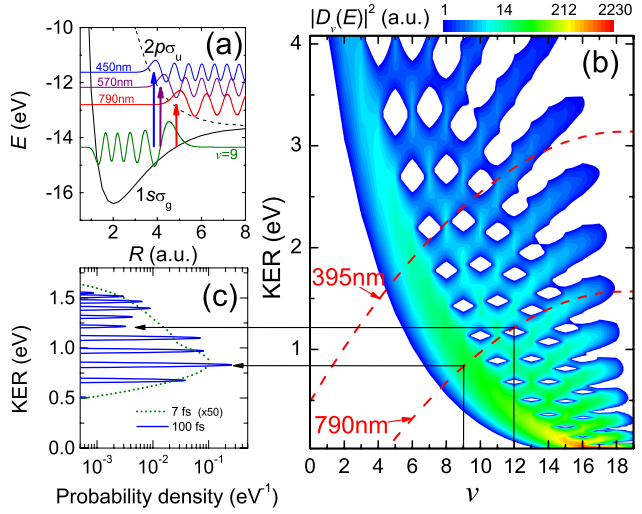


FIG. 1 (color online). (a) $H_2^+$ potentials and wave functions, see text. (b) Square of the amplitude of the $H_2^+$ dipole-matrix elements ($|D_v(E)|^2$) as a function of $v$ and KER. Curves shown for 790 and 395 nm are defined by KER $= E_v + \hbar\omega + 13.6$ eV. (c) $H_2^+$ dissociation probability density using perturbation theory ($4 \times 10^{10}$ W/cm$^2$) for 7 and 100 fs, 790 nm pulses, after Franck-Condon averaging.

with Fig. 1(b) shows that for $v = 9$, the dipole-matrix element is maximal at about 790 nm and oscillates under a decaying envelope with decreasing wavelength. The dips cause the dissociation suppression that we observe.

The dissociation probability $P_D$ from first-order time-dependent perturbation theory is related to the dipole-matrix elements by $P_D = \int \frac{dP}{dE} dE$, where in the rotating wave approximation (in atomic units)

$$\frac{dP_v}{dE} = \pi \frac{2\ln 2}{(\Delta\omega)^2} I |D_v(E)|^2 \exp\left[-\left(\frac{2\sqrt{\ln 2}(\omega - \omega_{\rm fi})}{\Delta\omega}\right)^2\right]. \quad (1)$$

In this expression, $I$ is the laser peak intensity, $\omega_{\rm fi} = E - E_v$, and $\Delta\omega$ is the laser bandwidth assuming a Gaussian envelope in time. Thus, the choice of $\omega$ acts as a filter on $D_v(E)$ as demonstrated in Fig. 1(b) for 395 and 790 nm.

From Fig. 1(b), we can make several predictions. For example, at 790 nm, we expect $P_D$ to be suppressed for $v = 12$ and 13 due to the minima in $|D_v(E)|^2$. Similarly, at 395 nm, we expect suppression for $v = 7$, 9, and 10. The laser bandwidth (pulse duration) determines the width of the frequency filter; hence, for very short pulses ($\lesssim$10 fs), we expect the vibrational peaks to merge in KER and smear out any visible suppression while for long pulses ($\gtrsim$100 fs), the suppressions will be well-defined.

Using Eq. (1) and $|D_v(E)|^2$ from Fig. 1(b), we check these predictions by plotting the KER spectrum from perturbation theory for 100 and 7 fs, 790 nm pulses in Fig. 1(c). The expected dips in probability for $v = 12$ and 13 are visible, reducing in contrast from 100 to 7 fs.

In reality, many laser-molecule experiments are performed in the strong-field ($\gtrsim 10^{12}$ W/cm$^2$) nonlinear regime. Thus, for the predictions of perturbation theory to be useful, they must survive to high intensities. Since the dipole-matrix elements determine the multiphoton transition rates, this is expected. Nonetheless, to explore the robustness of the dissociation suppression, we have recently developed a full-dimensional dissociation code that solves the time-dependent Schrödinger equation (TDSE) in the Born-Oppenheimer representation, including nuclear rotation, vibration, and electronic excitation, but neglecting the Coriolos and all nonadiabatic couplings [7]. See Ref. [19] for comparison of our theory with experiment on $H_2^+$. As ionization is omitted from the theory, we limit the intensities explored to below the ionization onset.

Figure 2(a) shows the KER distribution of $H_2^+$ (integrated over all angles) calculated using our intense-field theory for 790 nm, 45 fs, $4 \times 10^{12}$ W/cm$^2$ pulses, after Franck-Condon averaging. Distinct peaks are observed corresponding to one-photon dissociation of the $v$ states as indicated by the vibrational-comb ticks along the top of the plot, calculated from the field-free vibrational energies. The corresponding (nonweighted) $P_D$ for each $v$ state is shown in Fig. 2(c) along with the perturbation theory calculation. Clearly, a reduction in $P_D$ of $v = 12$ with respect to the neighboring states is predicted by the intense-field calculation, with the perturbation result in good qualitative agreement. This $v = 12$ suppression can also be found in the KER distribution in Fig. 2(a) by a dip (see arrow) at the $v = 12$ KER value (1.2 eV), and the magnitude of the dip suggests that it should be measurable

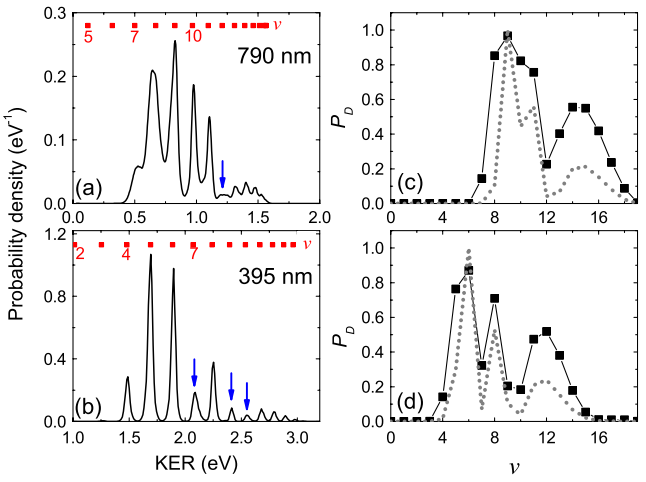


FIG. 2 (color online). Calculated kinetic energy release (KER) distributions of $H_2^+$ using 45 fs, $4 \times 10^{12}$ W/cm$^2$ pulses at (a) 790 nm and (b) 395 nm. Vibrational-comb ticks for one-photon dissociation are shown along the top of the panels. The corresponding dissociation probabilities $P_D$ are shown in (c) 790 nm and (d) 395 nm (solid points), as well as normalized perturbation results (dashed lines).

experimentally. Our calculations further reveal that the dissociation suppression persists at intensities at least up to $10^{13}$ W/cm$^2$ (the highest that we tested for 45 fs, and $10^{14}$ W/cm$^2$ for 7 fs)—albeit gradually reducing in contrast—and thus survives intensity-averaging due to the laser focal volume in an experiment. It is also present for all pulses that we have explored in the range 5–170 fs. Moreover, since our calculations account for nuclear rotation, these results show that this dissociation suppression is not washed out by rotation, unlike intensity-dependent stabilization and dynamical dissociation quenching [6,7,12].

As a check to ensure that the dissociation suppression is also measurable at other wavelengths, we repeated the calculations at 395 nm, the second-harmonic of a 790 nm Ti:Sapphire laser. The KER distribution and $P_D$ results are shown in Figs. 2(b) and 2(d), respectively. Significant suppression is observed for $v = 7$, 9, and 10, in agreement with the perturbation calculation. As with 790 nm, these suppressions can be seen in the KER distribution as amplitude dips at KER values of 2.1, 2.4, and 2.6 eV, respectively. Thus, the suppression does indeed persist for other wavelengths as predicted in Fig. 1(b).

A valuable check of this dissociation suppression is if we can observe it in the laboratory. For this purpose, we employed a coincidence three-dimensional momentum-imaging technique [20] involving a crossed-beams experiment of an ultrafast Ti:Sapphire laser focused onto a 5 keV ion-beam target of $H_2^+$. The importance of using an ion-beam target is that the ion source populates the $H_2^+$ molecules in a well-defined distribution of $v$ states (approximately Franck-Condon) by electron-impact ionization. In addition, the neutral fragments as well as ionic fragments can be measured in coincidence, giving kinematically complete information on dissociation and distinguishing this channel from ionization. This allows high-resolution KER and angular measurements whereby vibrationally resolved dissociation spectra can be achieved. Experimental details of the laser [21] and ion-beam [20,22] setups are described elsewhere.

The measured KER dissociation spectra of $H_2^+$ using 40 fs, $3 \times 10^{13}$ W/cm$^2$ pulses at 790 and 395 nm are shown in Figs. 3(a) and 3(b), respectively. The spectra are plotted for a $\pm 37°$ angular cut along the laser polarization to help reduce the effects of intensity averaging. Reasonably well resolved structures are observed at both wavelengths. The resolution is mostly limited by the position-sensitive detector (delay-line anode) resolution. These structures come from one-photon dissociation of $H_2^+$ $v$ states and agree well in KER with the field-free vibrational-comb energies (see ticks on plots).

To extract the relative $P_D$ values for the different $v$ states, we fit each of the peaks with Gaussian distributions as shown by the dashed curves in Figs. 3(a) and 3(b). The widths of all the Gaussians are fixed for each wavelength

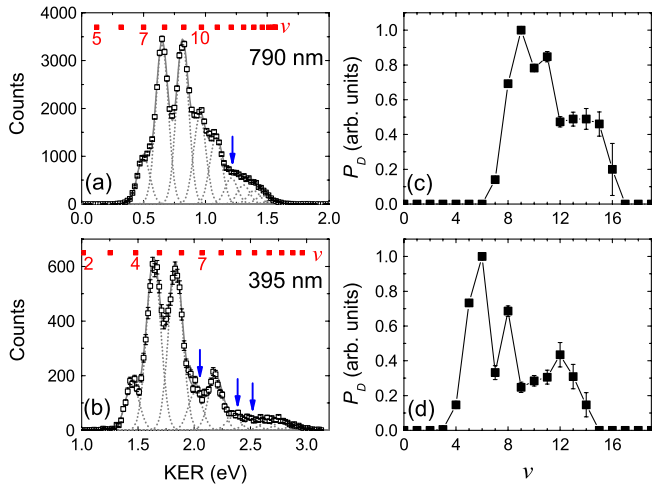


FIG. 3 (color online). Experimental kinetic energy release (KER) distributions of $H_2^+$ using 40 fs, $3 \times 10^{13}$ W/cm$^2$ pulses at (a) 790 nm and (b) 395 nm. Vibrational-comb ticks for one-photon dissociation are shown along the top of the panels. Error bars denote the statistical uncertainty. The corresponding relative dissociation probabilities $P_D$ are shown in (c) 790 nm and (d) 395 nm. Error bars are a sampling estimate of the uncertainty from the fitting procedure.

(FWHM = 0.12 eV for 790 nm; FWHM = 0.15 eV for 395 nm) to limit the number of free parameters. Also, their KER positions are restricted to a downward shift of $<3\%$ from the field-free vibrational energies. This small KER shift is likely to be caused by an energy scaling calibration uncertainty from our imaging setup. Essentially, the main remaining parameter is the amplitude of each peak which is adjusted to give the best overall fit (solid curve) to the data. The integrated area of each Gaussian distribution is then divided by the fractional Franck-Condon population of that $v$ state to give the relative $P_D$ value. The results are shown in Figs. 3(c) and 3(d) for 790 and 395 nm, respectively.

At 790 nm, a reduction in $P_D$ around $v = 12$ is observed. This suppression was predicted by our intense-field theory, and importantly, also by perturbation theory underlying its usefulness [Fig. 2(c)]. Similarly, 395 nm shows a reduction for $v = 7$ and around $v = 9$–11, again in good correspondence with our theory [Fig. 2(d)]. Overall, comparison of the theory and experiment in Figs. 2 and 3 show remarkable similarities in both the KER distributions and the $P_D$ plots despite the pulse durations, intensities (and intensity-averaging), and angular integration range all differing—in addition to the uncertainty from the experimental fitting procedure. The observed suppression in Fig. 3 is clear evidence that the suppression effect from the dipole coupling is measurable.

Finally, to push the limits of our test further, we repeated the 790 nm experiment for an $HD^+$ beam. This was to check the universal nature of the suppression for a more massive molecule whose initial $v$ wave functions differ

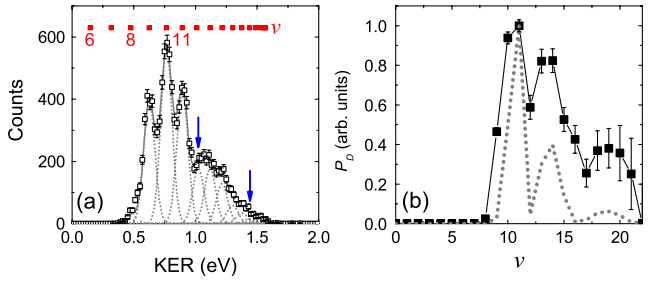


FIG. 4 (color online). Same as Figs. 3(a) and 3(c) for $HD^+$ dissociation into $H + D^+$ (the $H^+ + D$ channel is similar). The dashed line in (b) is a normalized perturbation calculation.

from those of $H_2^+$. The results, collected and analyzed in a similar manner to those in Fig. 3, are displayed in Fig. 4. Visible in the raw KER distribution [Fig. 4(a)] is a dip in yield at the $v = 12$ energy (1.0 eV). This dip shows up in the $P_D$ plot [Fig. 4(b)], as well as a second dip near $v = 17$. Comparison with perturbation theory for $HD^+$ [dashed curve in Fig. 4(b)] shows that both suppression dips are correctly predicted.

Briefly, we remark on the difference between this dipole-matrix element suppression and vibrational trapping. Vibrational trapping manifests from the formation of a laser-induced potential well above the one-photon (or three-photon) crossing in the adiabatic Floquet representation. Since the adiabatic Floquet representation is a strong-field multiphoton picture, the mechanism of vibrational trapping cannot be described by first-order perturbation theory, which is a weak-field single photon picture. The dipole-matrix element suppression, on the other hand, can adequately be described by perturbation theory as demonstrated here. Since the measurable effects of these two processes are similar, one must take care not to confuse them. Indeed, our findings question some of the value of vibrational trapping since many earlier observations can now be explained more effectively by the dipole-matrix element suppression.

We believe that mistaken identification of $H_2^+$ suppressed dissociation has occurred in the past. For example, in Fig. 4 of Ref. [8], the bound population of $H_2^+$ following interaction of 248, 355, and 532 nm pulses (83–177 fs) is plotted. Structure was observed whereby several $v$ states showed a higher bound population after the laser pulse than their neighbors. At the time, this was interpreted as due to vibrational trapping preventing these states from dissociating. Perturbation theory, based on the dipole-matrix elements, qualitatively reproduces the shape of the observed structure. Since vibrational trapping cannot be reproduced by perturbation theory, this suggests that the dipole-matrix elements are responsible for the structures in Ref. [8].

In summary, we have uncovered a vibrational suppression effect, explicitly studied for $H_2^+$, that is explained by a reduced dipole-matrix element coupling for certain $v$ states. Our theory shows that the effect is present for a broad range of intensities and pulse durations, and changes $v$ state for different laser frequencies. Most importantly, the effect has been observed experimentally, in good agreement with theory, using state-of-the-art experimental and theoretical techniques. This experimental realization has also been seen in $HD^+$ and may be similarly present in larger molecules although the additional degrees of freedom may make observation difficult.

In light of the predictive power we have found from the simple perturbation calculations, this offers an approach to theoretically studying large complex molecules. That is, molecular potentials and dipole couplings can be calculated using quantum-chemistry codes (e.g., GAMESS [23]), while perturbation theory can be straightforwardly performed for the complex systems to make basic qualitative predictions.

We thank Z. Chang and his group members and C. W. Fehrenbach for assistance with the laser and ion beams, respectively. Supported by the Chemical Sciences, Geosciences, and Biosciences Division, Office of Basic Energy Sciences, Office of Science, U.S. Department of Energy.

[1] K. Yamanouchi, Science **295**, 1659 (2002).
[2] J. H. Posthumus, Rep. Prog. Phys. **67**, 623 (2004).
[3] W. Demtröder, *Atoms, Molecules and Photons* (Springer, New York, 2006).
[4] A. D. Bandrauk and M. L. Sink, Chem. Phys. Lett. **57**, 569 (1978).
[5] E. E. Aubanel, J.-M. Gauthier, and A. D. Bandrauk, Phys. Rev. A **48**, 2145 (1993).
[6] E. E. Aubanel, A. Conjusteau, and A. D. Bandrauk, Phys. Rev. A **48**, R4011 (1993).
[7] F. Anis and B. D. Esry, Phys. Rev. A **77**, 033416 (2008).
[8] A. Giusti-Suzor and F. H. Mies, Phys. Rev. Lett. **68**, 3869 (1992).
[9] L. J. Frasinski *et al.*, Phys. Rev. Lett. **83**, 3625 (1999).
[10] J. H. Posthumus *et al.*, J. Phys. B **33**, L563 (2000).
[11] F. Châteauneuf *et al.*, J. Chem. Phys. **108**, 3974 (1998).
[12] H. Abou-Rachid, T.-T. Nguyen-Dang, and O. Atabek, J. Chem. Phys. **114**, 2197 (2001).
[13] M. Protopapas, C. H. Keitel, and P. L. Knight, Rep. Prog. Phys. **60**, 389 (1997).
[14] A. Giusti-Suzor *et al.*, J. Phys. B **28**, 309 (1995).
[15] A. Giusti-Suzor *et al.*, Phys. Rev. Lett. **64**, 515 (1990).
[16] P. H. Bucksbaum *et al.*, Phys. Rev. Lett. **64**, 1883 (1990).
[17] G. Jolicard and O. Atabek, Phys. Rev. A **46**, 5845 (1992).
[18] J. W. Cooper, Phys. Rev. **128**, 681 (1962).
[19] J. McKenna *et al.*, Phys. Rev. Lett. **100**, 133001 (2008).
[20] I. Ben-Itzhak *et al.*, Phys. Rev. Lett. **95**, 073002 (2005).
[21] H. Mashiko *et al.*, Appl. Phys. Lett. **90**, 161114 (2007).
[22] P. Q. Wang *et al.*, Phys. Rev. A **74**, 043411 (2006).
[23] M. W. Schmidt *et al.*, J. Comput. Chem. **14**, 1347 (1993).